

COHERENT ULTRAVIOLET RADIATION MEASUREMENTS OF LASER INDUCED BUNCHING IN A SEEDED FEL

M. Veronese*, A. Abrami, E. Allaria, M. Ferianis, E. Ferrari,
M. Trovò, Elettra-Sincrotrone Trieste, Trieste, Italy
F. Cianciosi, ESRF, Grenoble, France.

Abstract

Optimization of the bunching process in a seeded FEL like FERMI is an important aspect for machine operation. In this paper we discuss about the power detection of coherent radiation in the UV range as a valuable method for optimizing the bunching induced by the seeding process on the electron beam. Experimental results obtained at FERMI are presented here. Measurements of UV coherent transition and diffraction radiation have been used to quantify the bunching produced by the seed laser at lower laser harmonics. The dependence of the laser induced CUVTR signal on various parameters is experimentally studied. Future upgrades and possibilities for bunching measurements at shortest wavelengths are also discussed.

INTRODUCTION

FERMI is a seeded FEL operating in the spectral range from VUV to soft x-rays [1]. It is based on a SLAC/BLN/UCLA type RF-gun, a normal conducting LINAC, currently operated up to 1.4 GeV. Longitudinal compression is provided by two magnetic chicanes BC1 and BC2 (respectively at 300 MeV and 600 MeV). The FEL has two undulator chains, namely FEL1 and FEL2. The first, FEL1, is a single cascade HGHG seed system designed to provide hundreds of micro joules per pulse in the range from 100 nm to 20 nm. The second, FEL2, is a double cascade seeded system designed to reach 4 nm at the shortest wavelength. Optimization for a seeded FEL is a multi-parameter optimization process. To reach optimal FEL emission several conditions have to be met. One of the key points is to guarantee that the correct amount of bunching is produced. The bunching is the current modulation produced on the electron bunch by the combined action of the seed laser, the modulator undulator and the dispersive section. To guarantee optimal performance of the FEL the bunching has to be sufficiently large to produce high peak power FEL radiation but not too large, to avoid degradation of the power and spectral purity of the FEL. A diagnostics capable of measuring the amplitude of the bunching induced on the electron beam before the final radiator chain would be a very useful tool for machine tuning in seeded FELs especially for double or tripled cascaded FELs where the optimization is expected to be more critical. In principle the bunching could be derived from direct bunch profile measurements like the one performed using

e.g. deflecting cavities DCAV or Electro Optical Sampling (EOS) stations. However the bunching modulation has a small amplitude (usually $< 10\%$) and it occurs at short wavelengths. In these conditions DCAV and EOS are limited by SNR and resolution issues. In the paper we describe measurements made taking advantage of coherent radiation properties such as intensity and spectral selectivity. Coherent radiations have been exploited in many accelerator diagnostics for bunch length measurements in the mm-wave to THz wavelength range. More recently, coherent optical transition radiation (COTR) due to microbunching has been found impacting transverse profile measurements in several of the most recent FELs like LCLS, FERMI@Elettra and SACLA [2].

COHERENT RADIATIONS FOR A BUNCHING DIAGNOSTICS

A general description of coherent radiation properties can be found in [3]. The intensity depends on the square of the number of electrons involved in the bunching, thus greatly enhancing this radiation over the single particle emission. The spectral properties depend on the single particle spectral-angular distribution multiplied by the form factor squared. The form factor is the Fourier transform of the longitudinal bunch profile. In a seeded FEL by the energy modulation induced in the modulator undulator by the energy transfer from the seed laser to the electron beam is converted in density modulation by the dispersive section. Due to electron beam dynamics, the pure sinusoidal at the seed laser wavelength λ_s , is converted in a distribution similar to a saw tooth distribution. This means that its Fourier transform will have peaks at seed laser wavelength harmonics λ_s/n where n is an integer greater than 1. Moreover the bunching amplitude is exponentially damped at higher harmonics. This means that the coherent power emitted at these wavelengths is also expected to decrease as n increases. Considering the FERMI@Elettra case in standard operation the seeding wavelength is $\lambda_s^{FEL1} = 260$ nm. For FEL2 the second stage seeding usually occurs at the 8th harmonics i.e. at a wavelength $\lambda_s^{FEL2} = \lambda_s^{FEL1}/6 = 43.3$ nm. This means that the coherent radiation emitted by the bunching will be outside the visible spectral range with wavelengths extending from the ultraviolet (UV) to the vacuum ultraviolet (VUV) range. In the present paper we report measurement of transition radiation (TR) and diffraction radiation (DR). Since they are emitted coherently in the ultraviolet range we will refer to them respectively as

* marco.veronese@elettra.trieste.it

coherent ultraviolet transition radiation (CUVTR) and coherent ultraviolet diffraction radiation (CUVDR). Considering the single particle emission, in both cases the plasma wavelength plays a crucial role. For $\lambda \gg \lambda_p$ both forward and backward TR have about the same magnitude. For $\lambda \ll \lambda_p$ the backwards TR is strongly suppressed and only forward TR is emitted up to wavelengths of the order of λ_{cr} where $\lambda_{cr} = \lambda_p/\gamma$ [4]. The case of forward diffraction radiation has been studied by [5] also for $\lambda \ll \lambda_p$ and indicate a longer critical wavelength and a generally smaller intensity emitted from forward DR compared to forward TR. In our case, for standard aluminum foils λ_p is 37.8 nm [6] and the wavelength range of our interest, between 100 nm and 20 nm. With these parameters λ is neither much shorter nor much longer than λ_p and both approximated descriptions may not fully apply since the frequency dependence of the relative permittivity have to be fully considered. The spectral range of interest poses also a series of limitations in terms of radiation transport and detection. Moreover materials transmission becomes quickly and issue as the wavelength reaches UV and VUV, to the point were also the air absorption is not tolerable and filters (like aluminum foils) have to be chosen with a thickness below 1 micron to achieve a reasonable transmission. Finally in the VUV also the reflectivity has a dramatic dependence on the incidence angle. In using coherent radiations we gain on intensity since it has a quadratic dependence on the number of the electrons involved in the emission process. This effect increase greatly the emission intensity compensating to some extent the intensity drop due to the smaller number of electrons involved and the decrease in the radiation emission yield in the UV-VUV range compared to the visible.

EXPERIMENTAL LAYOUT

We have performed test measurements in the FERMI@Elettra FEL. The layout of the free electron laser in the undulator hall is depicted in Fig. 1. In the figure the beam travel from left to right and is depicted in yellow. The seed laser pulse is depicted in dark green, the modulator undulator (MOD) in red, while the dispersive section is in light green and the radiators (RAD) are in blue and violet. After the last radiator the electron beam travels towards bending dipoles that steers it to the main beam dump. To perform the experiments described in this paper

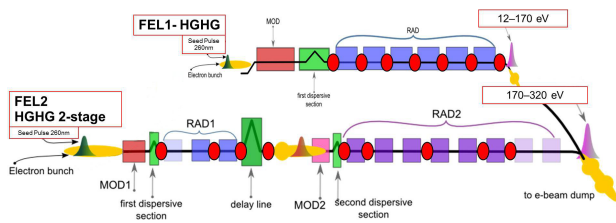


Figure 1: FERMI FEL1 and FEL2 layout.

dedicated for these development. The first, called MBSCR is installed between the last radiator and the first dipole. While the second, called PHSCR is installed on the straight line downstream the first dipole. We have tested the three configurations listed in Table 1 and depicted in Fig. 2. The

Table 1: Configuration Used in the Measurements

Layout	Emitter	Detector
A	double foil (TR FW)	Al coated photo diode
B	double foil (TR BW)	Al coated YAG:Ce
C	pinhole (DR FW)	Al coated photo diode

MBSCR has been equipped with the double-foil emitter and a pinhole that can be moved transversely into the beam. In the double foil emitter the 1st foil is a 1 μm thick aluminum foil set at normal incidence, while the 2nd foil is a 1 μm thick aluminum foil set at 45 deg of incidence angle. Below the second foil we have installed a YAG:Ce crystal coated with 100 nm of aluminum. The PHSCR is installed 16 m downstream the MBSCR and it is a multi-screen system equipped with several scintillators and an aluminum coated AXUV100 photo diode from IRD Inc. The photodiode is partially covered by a 3mm diameter pinhole. The photo diode signal is acquired by a Lecroy Wavesurfer MX 1GHz digital oscilloscope to allow for direct detection. We have tested the three configurations listed in Table 1.

In the double-foil arrangement the first surface of 1st

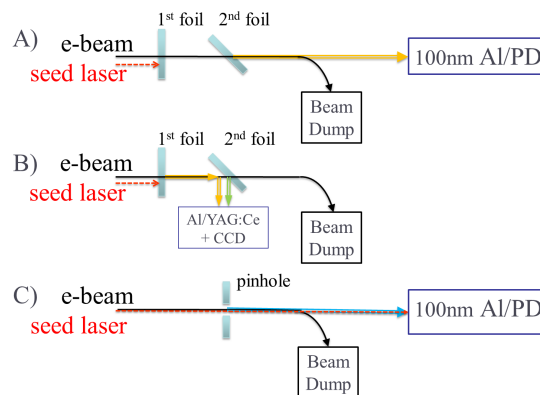


Figure 2: Experimental Layout.

foil is used to suppress unwanted seed laser radiation at 260nm. The second surface of the 1st foil emits forward transition radiation, while the first surface of the 2nd foil emits backward transition radiation and reflects the forwards radiation from the 1st. This is the source of radiation in layout B. The second surface of the 2nd foil emits forward radiation and is the source for radiation in scheme A. An aluminum plate with a transverse dimension of 19x19 mm and a hole of 2 mm diameter is the pinhole used in layout C as FW DR source. The aluminum coating of the photo diode is designed to act as a band pass filter in the wavelength range from approximately 17 nm to 80

nm with a transmission which is no flat but well above 20% in this whole range. The spectral response of the 100 nm Al coating of YAG:Ce used in scheme B, is also dominating the system spectral response and efficiency. From the above discussion it is clear the in all cases the measurement is performed on short wavelength harmonics with harmonic number $n > 3$. This is particularly interesting because similar measurements could be applied to the second stage of a double cascaded system whose seeding wavelength, taking FERMI FEL2 as an examples, is in the range 65-20 nm range. In all cases these measurement are better performed downstream of a bending magnet and are not online in the sense that have limited compatibility with an FEL operation because either the photo diode or the double foil will probably not withstand full power FEL flux density.

COHERENT UV TRANSITION RADIATION

We have tested the scheme A and applied it to the study of a few machine parameters. In Fig. 3 we show the CUVTR signal as a function of the seed laser temporal delay. In Fig. 4 we show the CUVTR as a function of seed laser

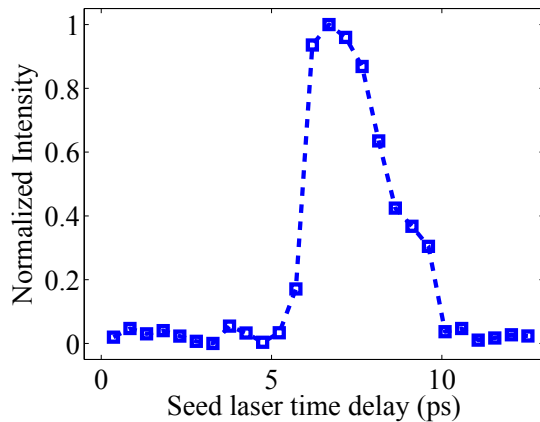


Figure 3: CUVTR intensity measured as a function of the seed laser time delay.

attenuator angle. The seed laser power in this range of attenuation is inversely proportional to the attenuator angle. In Fig. 5 we report the behavior of the CUVTR signal as a function of the dispersive section current. The dispersion R_{56} increases with the dispersive magnets current. The two curves in the figure were acquired for different setting of the seed laser power. The angle of 63.8 deg corresponds to a lower seed power while the angle of 61 deg corresponds to a higher seed power. The signal (i.e. the bunching) is shifted towards higher dispersive section currents (higher R_{56}) in the case of lower seed power. This means that to produce the same amount of bunching with a lower seed power energy you have to increase the dispersive section current, as expected by the electron beam dynamics of the bunching section. It is worth noting that the above measurement are averages of five acquisitions. We attempted

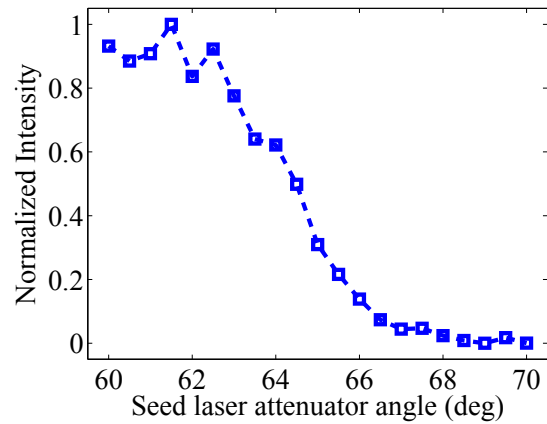


Figure 4: CUVTR intensity measured as a function of the seed laser power.

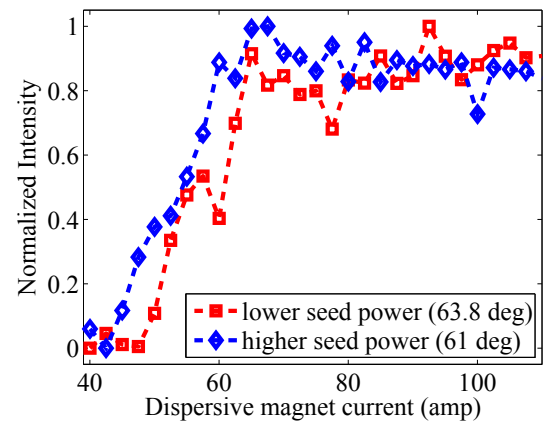


Figure 5: CUVTR intensity as a function of the dispersive section current for different values of seed laser power.

using scheme B. This scheme is similar to ordinary OTR diagnostics geometry but is more complex from the point of view of involved radiations. The second surface of the 1st foil will emit forward TR which is then reflected by the second foil, the first surface of the 2nd foil will emit backward TR and the two will also interfere to some extent. We used a 100 nm aluminized YAG:Ce crystal to convert UV radiation into visible while suppressing other unwanted COTR visible radiations. With our standard multi-screen optical systems (SIGMA 105 lens f2.8 and Basler Scout 1300-32gm CCD camera) we could not detect any signal even averaging over multiple shots. Backward TR is expected to be weak. Forward TR in this arrangement is most probably suppressed by the UV reflectivity of Al at 45deg which is of the order of 1% at 40nm [7]. The expected transmission of the 100 nm aluminum thin film is expected to play a minor role within the transmission bandwidth.

COHERENT UV DIFFRACTION RADIATION

We have repeated the measurements of CUVTR with another source of radiation: forward diffraction radiation (scheme C of Fig.2). The DR source is the pinhole installed in the MBSCR screen, used it in conjunction with aluminized photodiode as in the TR measurements. In Fig.6

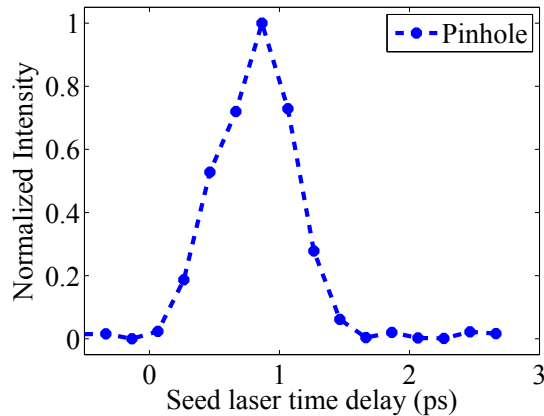


Figure 6: CUVDR intensity measured as a function of the seed laser time delay.

we report the signal dependence on the seed laser time delay, while in Fig.7 we report the CUVDR dependence on the seed laser power. It can be seen comparing to Fig. 3, 4 that the measurements show similar qualitative behavior. A direct comparison between CUVTR and CUVDR

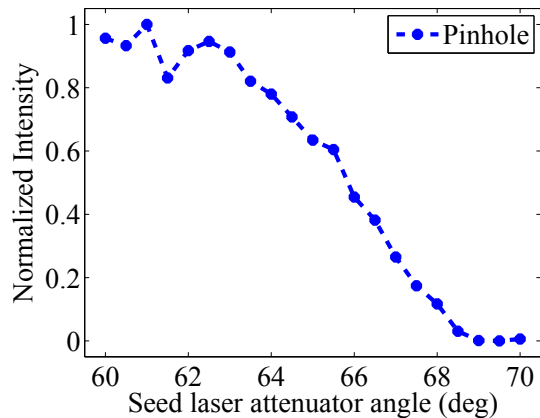


Figure 7: CUVDR intensity measured as a function of the seed laser power.

data is difficult, since they were not performed with exactly the same machine conditions. For the CUVTR measurements the charge was 390 pC and the bunch duration 2.5 ps FWHM compared to 500 pC and 0.8 ps FWHM in the case of the CUVDR. A qualitative comparison shows that to obtain a similar SNR for CUVDR data we needed to average over six times more bunches (30 consecutive bunches, compared to 5 in the case of CUVTR).

ISBN 978-3-95450-127-4

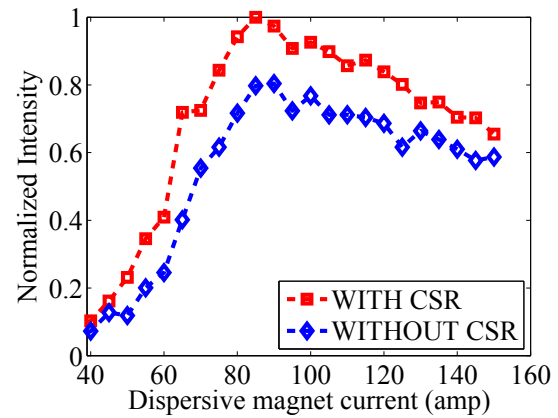


Figure 8: CUVDR intensity measured as a function of the dispersive section current. The red signal is CUVTR + CSR, while the blue is CUVTR only.

Finally we report the dependence of coherent diffraction radiation on the dispersive section. In Fig. 8 we show two curves for comparison. The red curve is obtained with the standard measurement, while the blue one is obtained steering before it enters the bending magnet to remove contributions from coherent synchrotron radiation (CSR). From the figure it is clear that although a contribution from CSR is present the CUVDR is dominating the standard measurement. Finally future new arrangements have to be devised to improve the compatibility of such a diagnostic with machine operation. These may include the use of ionization monitors and/or coherent synchrotron radiation as a source.

ACKNOWLEDGMENTS

We would like to thank T.Noohnan and D.Walters of Argonne National Laboratory and T. Borden now at FRIB, Michigan State University for the initial mechanical design of the MBSCR system. This work was supported in part by the Italian Ministry of University and Research under grants FIRB-RBAP045JF2 and FIRB-RBAP-6AWK3.

REFERENCES

- [1] E. Allaria *et al.*, "Nature Photonics advance online publication", 23 September 2012, (doi:10.1038/nphoton.2012.233).
- [2] J. Frisch *et al.* THBAU01, Proceedings of FEL2008, Gyeongju, Korea, (2008).
- [3] O. Grimm, TESLA-FEL Report 2008-05, Hamburg, (2008).
- [4] B. Jitter, CAA-TECH-NOTE-internal-24, (1992).
- [5] A. A. Tishchenko *et al.*, "Phys. Rev. E", v. 70, pg. 066501, (2004).
- [6] B. Dolgoshein, "Nucl. Instrum. Met. Phys. Res. A", v. 326, pg. 434, (1992).
- [7] CXRO, "X-Ray Interactions With Matter", http://henke.lbl.gov/optical_constants.